Explainable DL models in lung cancer using CLIP

Joel Bautista Rodríguez

Resum—Resum del projecte, màxim 10 línies. ....
....
....
....
....
....
....
....
....
....

Paraules clau—Paraules clau del projecte, màxim 2 línies. ....
....

Abstract—Versió en anglès del resum. ....
....
....
....
....
....
....
....
....
....

Index Terms—Versió en anglès de les paraules clau. ....
....

1 Introduction – Work Context

Lung cancer detection using deep learning (DL) has shown remarkable advancements in recent years, leveraging powerful models that extract meaningful patterns from medical images. However, one of the major challenges in medical AI applications remains the lack of interpretability, as deep learning models often operate as *black boxes*, making it difficult for clinicians to trust and validate their decisions. To address this, explainable deep learning (XDL) approaches are essential to bridge the gap between AI-generated predictions and medical reasoning. This project focuses on leveraging CLIP to enhance explainability in lung cancer detection models. CLIP is a multimodal model capable of learning a shared latent space where images and textual descriptions are aligned**[8]**. While traditional deep learning models rely solely on image-based features, CLIP introduces a language-guided approach, enabling the association of lung cancer imaging data with medical reports. This allows for a more intuitive and interpretable decision-making process, aligning with the need for transparency in medical AI applications.

To achieve this, the project builds upon an existing lung cancer detection model that has already been trained to extract the most relevant visual features from radiological images. The primary goal is to extend this by effectively extracting and structuring features from medical reports, ensuring that textual and visual embeddings are properly aligned within a shared latent space. This is crucial for making CLIP fully functional in this specific medical application, as it ensures that the model learns the correct relationships between medical images and their corresponding diagnostic descriptions.

2 State of the Art

2.1 Medical Image Captioning and Report Generation

Nowadays, the automatic generation of medical reports from radiological images has emerged as a crucial area in medical AI **[1][2]**, with the purpose to bridge the gap between computer vision and natural language processing (NLP). The main goal is to translate visual medical data into accurate textual descriptions, enhancing diagnostic efficiency and reducing the workload of radi-

ologists and clinicians. Retrieval-based and template-based approaches have been traditionally used but, in the last years, gradually replaced by deep learning (DL) - based generative models**[5][9]**, which allow for more flexible context-aware, and detailed medical report generation.

Thus, delving into deep learning-based methods for medical image captioning, modern approaches employ deep learning architectures to automate diagnostic report generation. These models generally adhere to an encoder-decoder paradigm**[9]**, categorized into three main types:

- CNN-Based Encoders: these use Convolutional Neural Networks (CNNs) like ResNet, EfficientNet, and Vision Transformers (ViTs) to extract meaningful visual features from medical images.
- RNN-Based Decoders: recurrent models such as RNNs, LSTMs, and Transformer-based architectures process these visual features to generate coherent textual descriptions.
- Attention Mechanisms: these enhance caption relevance by directing focus to the most critical image regions during text generation**[3].**

As mentioned, explainability is crucial actually because deep learning models must justify their decisions to gain tust from healthcare professionals. This is where CLIP and similar multimodal approaches play a vital role.

2.2 CLIP: A Game Changer in Medical AI

CLIP, developed by OpenAI, is a vision-language model designed to understand both images and text by jointly training on image-text pairs. CLIP is pre-trained on vast amounts of image-text pairs from the internet using contrastive learning**[3]**.

The way it works can be simplified to 3 steps:

1. Feature Extraction: CLIP encodes images and text separately using a VIsion Transformer (ViT) for images and a Transformer-based text encoder.

2. Latent Space Alignment: Both encoders project their outputs into a shared embedding space, where semantically related images and texts are pulled closer together**[4]**.

3. Zero-Shot Learning: Unlike traditional models that require fine-tuning on domain-specific datasets, CLIP is capable to classify images and generate text descriptions without retraining, making it highly adaptable to medical imaging tasks such as lung cancer detection, hematology and pathology (PLIP and BiomedCLIP), radiology report generation.

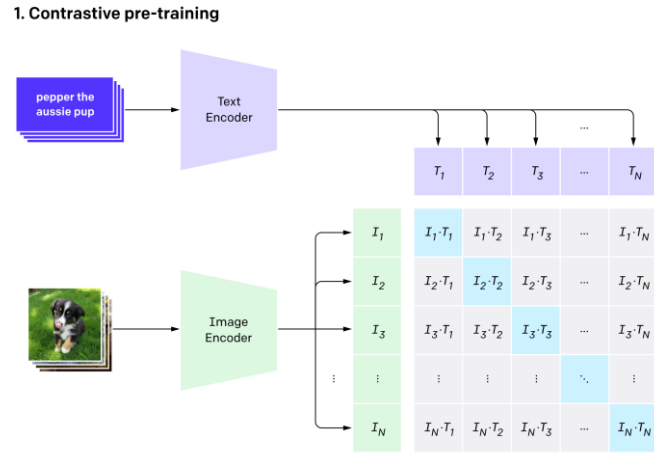

Figure 1. Contrastive pre-training

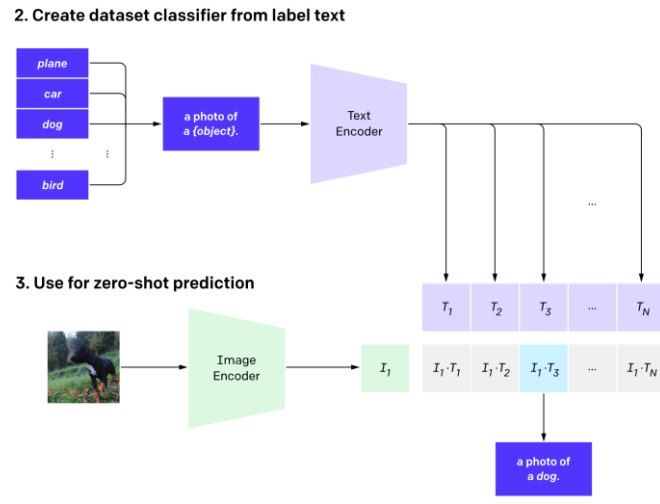

Figure 2. Dataset classifier from label text and zero-shot prediction

3 OBJECTIVES

The primary objective of this project is to enhance the explainability and interpretability of deep learning models for lung cancer detection by integrating medical image and diagnostic text embeddings into a shared latent space using CLIP-based architectures. This approach aims to create a more transparent and clinically relevant AI system that effectively aligns radiological images with textual medical diagnoses through contrastive learning.
A critical aspect of the project is modifying or adapting an existing CLIP architecture to integrate both the image encoder and the text encoder into a joint embedding space. Through contrastive learning, the model will be trained to maximize the similarity between images and their corresponding medical reports while increasing the distance between unrelated image-text pairs. To optimize this process, the contrastive loss function will be fine-tuned, ensuring that the alignment between visual and textual modalities is precise and meaningful in a medical context.

4 METODOLOGY AND PLANIFICATION

The project followed an *Agile methodology*, specifically applying the *Kanban approach* to manage workflow efficiently. For this purpose, the tool **Trello** was used to plan, organize, and monitor the progress of tasks throughout the project. This approach allowed for a clear visualization of task status, helped prioritize activities, and supported a flexible and iterative development process.

5 DATA EXPLORATION

The data used comprises both radiological and clinical metadata extracted from annotated CT scans. On one hand, it includes pre-extracted image features that capture the texture of the CT scans on a per-slice basis. For each slice there is a feature vector and metadata, as well as an additional vector capturing intensity-related information. On the other hand, the dataset contains structured metadata which contains patient specific radiological descriptors.

In fact, for the training and evaluating the models, a subset of five clinically relevant variables was selected from this metadata: *nodule shape*, *nodule density*, *vinfiltration*, *cdiff* (cell differentiation) and *necrosis*.

5.1 Statistical Study of Radiologic Descriptors

To explore the structure and dependencies within the selected variables, variety of statistical indicators and visualizations were employed.

As a first step, the distribution of each selected variable was analyzed. Overall, the categorical variables displayed a clear imbalance across their classes. Among them, *vinfiltration* showed the most pronounced imbalance (see Figure 3). Otherwise, *nodule shape* showed the most balanced distribution as it can be observed in Figure 4.

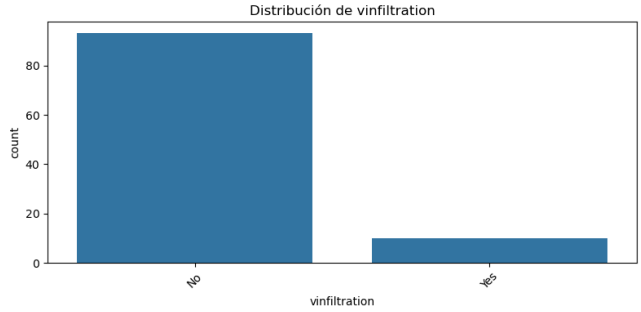

Figure 3. VInfiltration label distribution

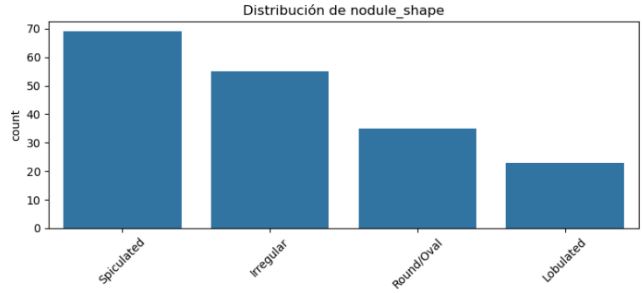

Figure 4. Nodule Shape label distribution

This imbalance is important to consider during model training and evaluation, as it may influence the classifier's sensitivity to minority classes.

In order to explore potential dependencies between variables, both *Chi-square* statistics and *Cramér's V* correlations were calculated across the descriptors. As shown in Figure 5, the χ^2 heatmap highlights notably strong associations between nodule shape and cdiff ($\chi^2 = 11$), as well as between nodule density and cdiff ($\chi^2 = 22$). This suggests that non-random associations may reflect underlying clinical or radiological patterns.

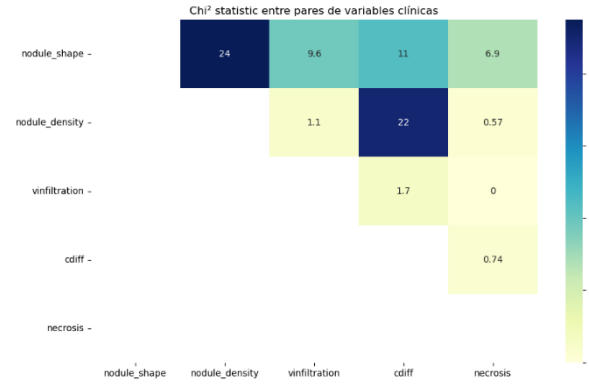

Figure 5. Chi-square heatmap

These findings are supported by the *Cramer's V* correlation matrix (Figure 6), where the strongest correlations also are between nodule density and cdiff (0.30).

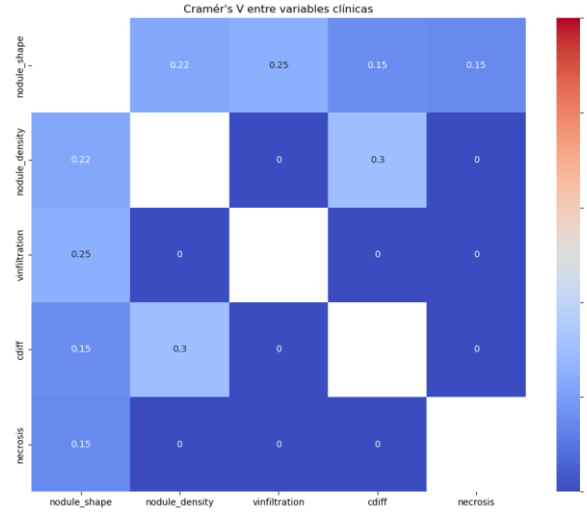

Figure 6. Cramer's V correlation matrix

6 DEVELOPMENT

6.1 Architecture

To address the task of learning meaningful representations from both radiological image features and structured metadata, a multimodal neural architecture referred to as *CLIPMedical*, was implemented.

First, the clinical metadata is processed using a frozen ClinicalBERT transformer. Then, token embeddings extracted from ClinicalBERT are projected to a lower-dimensional space (from 768 to 512 dimensions) via learnable linear layer. Next, a multi-head self-attention mechanism is applied to model dependencies between the tokens, theorically producing a contextualized representation of the input descriptors (see Figure 7).

On the other side, image features are represented as 1024-dimensional vectors and passed through a feedforward projection layer consisting of a linear transformation, ReLU activation, and layer normalization. This has the objective to map the image embeddings into the same 512-dimensional latent space as the text embeddings (see Figure 7).

The fusion of modalities is performed using contrastive alignment, where image and text embeddings are normalized and compared using Euclidean distance. The model outputs a similarity matrix between batch-wise image and text representations, promoting alignment of matched image-text pairs (see Figure 7).

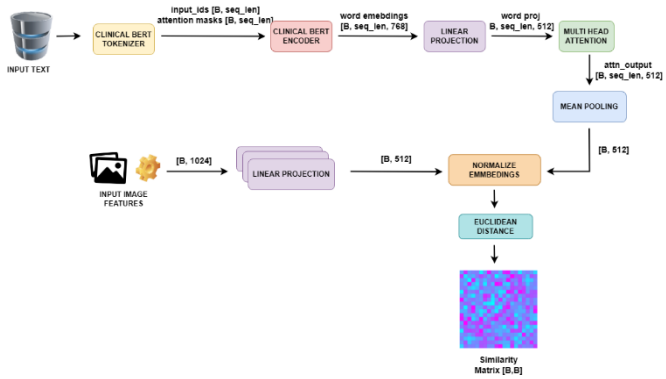

Figure 7. Architecture Schema

6.2 Model Training

The training phase of the model is based on a contrastive learning approach, where the goal is to align clinical text descriptors with their corresponding image features in a shared embedding space. In addition, the model is trained in batches using paired samples, and optimization is guided by a contrastive *cross-entropy loss* that is explained below.

Each training batch starts with the construction of paried inputs. A batch of image feature vectors, each of image feature vectors is passed through a learnable projection head which results in a set of projected image embeddings of shape [B,512]. In parallel, the corresponding radiological descriptions already tokenized are processed by a frozen ClinicalBert encoder producing embeddings that are then pooled to obtain a final text representation of shape [B, 512].

All in a row, both the image and text embeddings are normalized, mapping them onto a unit hyperspace. This normalization step ensures that both cosine similarity and Euclidean distance can be interpreted in a comparable way for contrastive optimization.

Later, a pairwise distance matrix is computed across all image-text pairs in the batch. Specifically, the Euclidean distance is calculated between ecach image embedding and text embedding, resulting in a logits matrix of shape [B,B]. In this matrix, the entry at position *logits[i][j]* corresponds to the distance between the *i-th* image and the *j-th* text. These distances are later negated and scaled by a learnable temperature parameter.

The target labels for this training step are derived from the assumption that the *i.th* image in the batch corresoinds exactly to the *i-th* text. With the logits matrix and corresponding labels in hand, the model is trained using a *cross-entropy loss*, which encourages the similarity score of matching pairs to be maximized while penalizing similarity with the wrong pairs.

Finally, gradients are computed via backpropagation, and model parameters are updated using the Adam optimizer. This training loop explained above is repeated for each bach across multiple epochs.

6.3 Test & Evaluation

Once the model has been trained on a given fold, the evaluation phase begins by encoding and comparing test samples against a reference "catalog" constructed from the training data. This catalog serves as a fixed repository of text embeddings, allowing the model to retrieve the most semantically similar clinical descriptions for each unseen image.

To build this catalog, all text samples from the training set are decoded, tokenized and passed through the model's text encoder. A single 512-dimensional vector is obtained for each text, forming a matrix of embeddings that represents the reference catalog.

For inference, the model processes each test image feature vector which is projected into a normalized 512-dimensional embedding. Then, this embedding is compared to all entries in the catalog using cosine similarity, producing a ranked list of the most similar training texts. From the list, only the top-1 prediction is used for evaluation metrics.

First, a qualitative evaluation is used to check whether te correct text is present among the top-k predictions for each patient. Second, each predicted text is parsed to extract its radiological descriptors which are also compared against the ground-truth descriptors for that sample. Then, a confusion matrix is generated, showing classification performance across categories (see Figure 9).

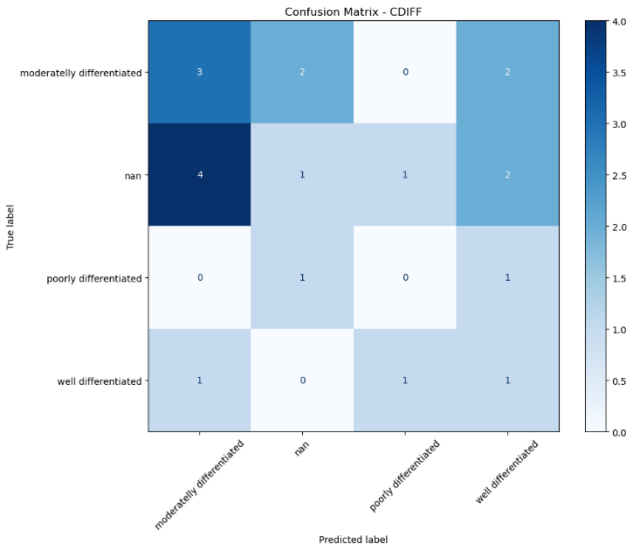

Figure 9. CDiff Confussion Matrix

Finally, the quantitative performance is measured using standard classification metrics. Precision, recall, f1-score and accuracy are computed for each radiological descriptor on the top-1 predicted text. These metrics are computed for each fold and then aggregated across folds to obtain an overall performance summary. All results are saved to CSV files and plotted using boxplots, as seen in Figure 10.

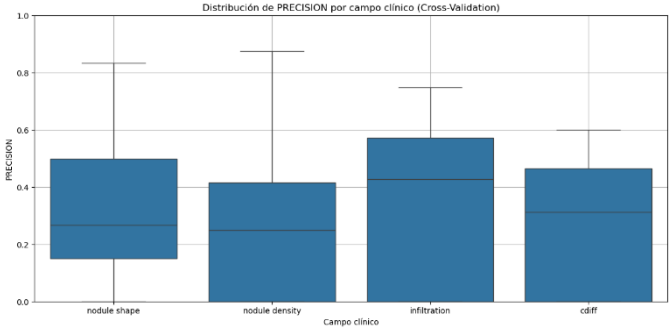

Figure 10. Precision for each descriptor across all folds

7 EXPERIMENTAL DESIGN

This experimental setup is designed to evaluate the performance and generalizability of the *CLIPMedical* in the task of aligning clinical text descriptors and imatge-derived features.

To this end, as explained in the data exploration section, a multi-hospital data set was used, combining annotated cases from Can Ruti, Del Mar, and Mutua Terrassa. For all the experiments, the same five radiological descriptors explained before were selected.

To ensure robust evaluation, the experimental protocol followed a 5-fold cross validation strategy. For each fold, a new model instance was trained from scratch. Stratification was not enforced, but folds were randomly sampled to reduce potential class bias.

Each experiments has itself a set of paràmetres, which are selected to explore how the model performs with the changes in any of them. These parameters include the batch size, number of epochs, pre-trained extractor used, learning rate and optimizer, among others. Before presenting each experiment, the specific configuration used will be explicitly stated to provide clarity.

8 PRE-TRAINED EXTRACTORS COMPARATIVE

The configuration of parameters used for training and evaluation in the following experiments is summarized in Table 1.

Parameter	*Value*
Batch size	64
Epochs	30
Learning rate	$1x10^{-4}$
Optimizer	Adam
Loss function	Cross-Entropy Loss
Tokenizer	ClinicalBERT
Text Encoder output	768 → 512
Image Encoder output	1024 → 512
Evaluation Strategy	Top-1 retrieval + per field metrics

Table 1. Parameters Configuration

8.1 ResNet18

The evaluation of the model using imatge features extracted from a pretrained ResNet18 revealed generally poor performance. The overall predictive capacity was low, and results varied considerably across clinical fields.

Globally, infiltration was the descriptor with te highest stability and overall F1-score, showing a median above 0.35 but without compact interquartile range. On the other hand, nodule density and cdiff showed more dispersion and lower median vàlues, indicating inconsistent prediction quality across folds. This can be promoted in part by class imbalance, especially in the case of cdiff, where "poorly differentiated " yielded very low precision (0.10) and recalll (0.17), as shown in figures 11, 12 and 13.

From a recall perspective (Figure 11), nodule shape and infiltration reached the broadest range, with some folds achieving values above 0.70. However, these high scores are not sustained consistently, as reflected in the wider spred of the boxplots.

When looking at the overall F1-score distribution (Figure 13), infiltration and nodule shape appear to be the most learnable and consistently predictable fields, while cdiff

continues to reflect the impact of low recall in minority classes. In particular, the standard deviation for "well differentiated" in cdiff is high, indicating inconsistent behavior across folds.

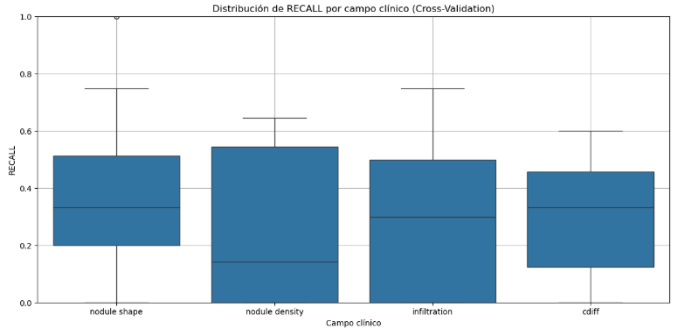

Figure 11. Recall boxplots by field

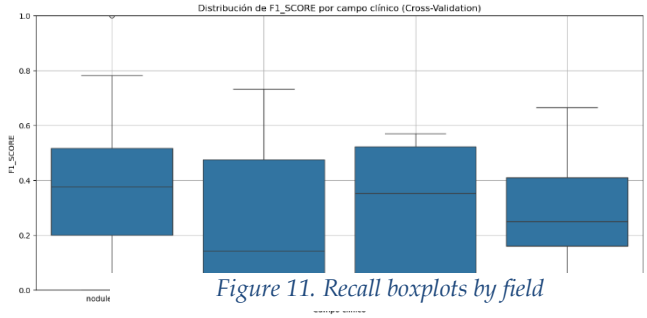

Figure 12. F1-score boxplots by field

8.2 ResNet152

8.3 MobileNetV2

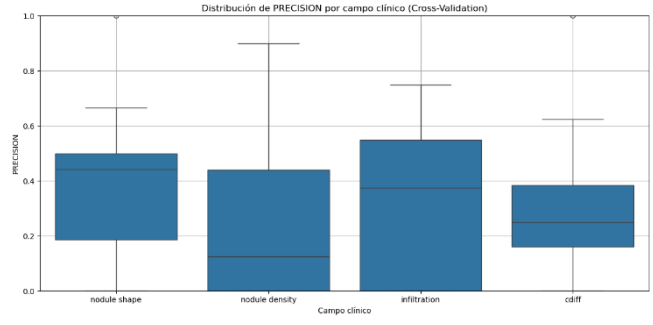

Figure 13. Precision boxplots by field

3 CONCLUSIÓ

....

AGRAÏMENTS

....

BIBLIOGRAFIA

[1] Referència 1
[2] Referència 2
[3] Etc.

APÈNDIX

A1. SECCIÓ D'APÈNDIX

....

A2. SECCIÓ D'APÈNDIX

....